Journal of Sound and Vibration (1998) **209**(1), 187–198

LETTERS TO THE EDITOR

AVERAGING AND BIFURCATIONS IN AN OSCILLATOR WITH A HISTORY DEPENDENT RESTORING FORCE

Y. KETEMA

Department of Aerospace Engineering and Mechanics, University of Minnesota, Minneapolis, Minnesota 55455, *U.S.A.*

(*Received* 5 *February* 1997, *and in final form* 21 *July* 1997)

1. INTRODUCTION

Viscoelastic materials have widespread application in the area of vibration damping and isolation. Such applications include the damping of vibrations in flexible structures such as beams, plates, etc. (see e.g. references [1–4]). In addition, such materials are often used in mechanical systems consisting of discrete components, where they provide vibration isolation and damping. For example, viscoelastic materials are common elements in machine systems (see references [1, 5]).

The mechanical properties of viscoelastic materials are characterized by a time dependent relationship between stress and strain. Hence, the state of stress at a point in a viscoelastic material depends on the history of the state of strain at that point, as well as on the current state of strain. For this reason, a viscoelastic material may also be referred to as a *material with memory*. In addition, if the relative deformations of the recent past are more important in determining the stresses at a point than those further back in time, the material is said to have *fading memory* (see e.g. references [6] and [7]). When the material-with-memory model is used in its simplest form, the viscoelastic material may be characterized by its relaxation modulus, which gives the overall strength of the history dependence, and one or more relaxation times, which govern the rate of fading of memory.

The material-with-memory model, with one relaxation time, was used to investigate the dynamics of a one-degree-of-freedom linear oscillator with a viscoelastic restoring force in reference [8]. The role of the relaxation time and the relaxation modulus in the vibration damping characteristics of the viscoelastic material was investigated, and conditions for optimal damping in the case of unforced oscillations were derived. Also, the response of the oscillator to sinusoidal forcing was studied.

Discrete mechanical models consisting of springs and dashpots are sometimes used in modelling viscoelastic forces. The simplest of these are the Voigt model, the Maxwell model, and the three element model (see e.g. reference [9]). These models, though they may give good qualitative descriptions of viscoelastic behavior, are not always adequate for practical purposes. Therefore, in applied studies of vibrations with viscoelastic forces, experimentally obtained frequency dependent complex moduli are often employed (see e.g. reference [1]). Both approaches—the mechanical models and the complex moduli—are only good for the case of linear, i.e. small, vibrations.

In the case of large vibrations, the non-linear history dependence of the viscoelastic force on the vibrational motion must be taken into consideration. This may be done by the use of the material-with-memory model. Thus, for example in reference [10] non-linear motions of an oscillator with viscoelastic restoring force were studied using the material-with-memory model. Based on Melnikov's method for subharmonic orbits (see e.g. reference [11]), a method was derived to determine the existence of non-linear

0022–460X/98/010187 + 12 $25.00/0/sv971237

periodic orbits, (subharmonic orbits), for the viscoelastic oscillator under the assumption of a small relaxation modulus. Also, an experimental method of dynamically measuring the relaxation time and relaxation modulus was suggested.

The main purpose of the present paper is to investigate the effects of the non-linearity in the history dependence of the force from a viscoelastic material, on the dynamics of a one-degree-of-freedom oscillator (see Figure 1). In section 2, the material-with-memory model used for the viscoelastic material is described and the dynamic equations for the oscillator are derived. It is shown that, though the oscillator has one degree of freedom, it is described by a three dimensional state space due to the history dependent force. In sections 3 and 4 the motion of the oscillator is studied. It is demonstrated how the governing equations may be put into a form that allows for the method of averaging to be applied, in order to study amplitude–frequency relationships for non-linear periodic motions. By the use of the method of averaging, it is shown that the non-linearity in the dissipative history dependent force may lead to a jump bifurcation in the oscillator even when the elastic part of the restoring force is linear.

2. CONSTITUTIVE MODEL AND DYNAMICAL EQUATIONS

In the main body of this work, the motion of a one-degree-of-freedom oscillator with a lumped mass m, which is subject to a restoring force due to the action of a viscoelastic material with memory and a force $p(\tau)$, where τ denotes time, will be studied. One adopts the same constitutive model as in reference [8] and assume that the motion and all forces are uniaxial, as indicated in Figure 1.

For the one-dimensional setting of Figure 1, let $x = \chi(X, \tau)$ denote the position at the present time τ of a particle of the viscoelastic bar which is at $X = \chi(X, 0)$ in its undistorted natural state at time $\tau = 0$. The history of the motion is represented by $\chi(X, \tau - s)$, $\forall s \geqslant 0$. Then, if one lets $F \equiv \partial\chi/\partial X$ denote the deformation gradient, the relative deformation gradient history is given by $F(X, \tau - s)/F(X, \tau)$, $\forall s \geqslant 0$. The relative history is then characterized by

$$J_\tau(X, \tau - s) = [F(X, \tau - s)]^2/[F(X, \tau)]^2 - 1, \qquad \forall s \geqslant 0. \tag{1}$$

The constitutive response function for determining the present value of the axial force $f(X, \tau)$ on the particle X in the viscoelastic bar is assumed to be of the finite-linear form, see reference [12]),

$$f(X, \tau) = \bar{f}^e(F(X, \tau)) + \int_0^\infty \dot{G}(s) J_\tau(X, \tau - s)\, \mathrm{d}s, \tag{2}$$

where $\bar{f}^e(\cdot)$ denotes the elastic response function and $G(\cdot)$ is the viscoelastic relaxation kernel for the material.

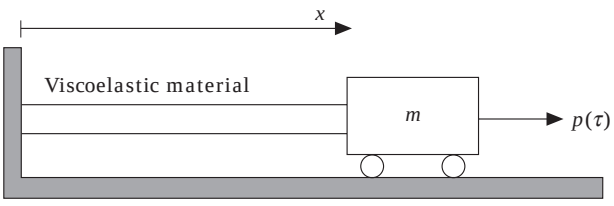

Figure 1. Schematic diagram of an one-degree-of-freedom oscillator with history type force.

One supposes that the motion of the viscoelastic bar is homogeneous, so that one may write

$$x = \chi(X, \tau) = X\tilde{x}(\tau). \tag{3}$$

Then, the deformation gradient $F(X, \tau) = \partial\chi(X, \tau)/\partial X = \tilde{x}(\tau)$ is, in fact, the homogeneous "stretch" of material filaments so that

$$\bar{f}^e(F(X, \tau)) = \bar{f}^e(\tilde{x}(\tau)), \qquad J_t(X, \tau - s) = [\tilde{x}^2(\tau - s) - \tilde{x}^2(\tau)]/\tilde{x}^2(\tau). \tag{4}$$

We shall assume that $G(\cdot)$ is given by the exponentially decaying relaxation function

$$G(s) \equiv G_0 e^{-s/\gamma}, \qquad \forall s \geqslant 0, \tag{5}$$

where $G_0 > 0$ and the relaxation time $\gamma > 0$. If one lets L_0 denote the referential length of the viscoelastic bar, then the dynamical equation for the mass m is

$$m\ddot{\chi}(L_0, \tau) = p(\tau) - f(L_0, \tau), \tag{6}$$

which, with equations (1), (3), and (4), can be rewritten as

$$mL_0\,\ddot{\tilde{x}}(\tau) = -\bar{f}^e(\tilde{x}(\tau)) + \frac{G_0}{\gamma}\int_0^\infty e^{-s/\gamma}\,\frac{\tilde{x}^2(\tau - s) - \tilde{x}^2(\tau)}{\tilde{x}^2(\tau)}\,\mathrm{d}s + P\cos(\Omega\tau), \tag{7}$$

where the special forcing function $p(\tau) = P\cos\Omega\tau$ has been introduced.

In the present work, it is convenient to rewrite equation (7) as a system of first order ordinary differential equations. To do this, one defines the auxiliary function

$$\tilde{\zeta}(\tau) = \int_0^\infty e^{-s/\gamma}\,\frac{\tilde{x}^2(\tau - s) - \tilde{x}^2(\tau)}{\tilde{x}^2(\tau)}\,\mathrm{d}s. \tag{8}$$

Then, it readily follows that equation (7) has the equivalent form

$$\dot{\tilde{x}}(\tau) = \tilde{\eta}(\tau), \qquad mL_0\,\dot{\tilde{\eta}}(\tau) = -\bar{f}^e(\tilde{x}(\tau)) + (G_0/\gamma)\tilde{\zeta}(\tau) + P\cos(\Omega\tau),$$
$$\dot{\tilde{\zeta}}(\tau) = -[1/\gamma + 2\tilde{\eta}(\tau)/\tilde{x}(\tau)]\tilde{\zeta}(\tau) - \gamma 2\tilde{\eta}(\tau)/\tilde{x}(\tau). \tag{9}$$

Clearly, an equilibrium point $(\tilde{x}^*, \tilde{\eta}^*, \tilde{\zeta}^*)$ for equations (9), (i.e. when $P = 0$), is given by $(\tilde{x}^*, 0, 0)$, where $\tilde{x}^*$ is any root of the equation $\bar{f}^e(\tilde{x}^*) = 0$.

In order to bring equations (9) into a dimensionless form, one defines a dimensionless time t through

$$t = \omega_0\,\tau, \tag{10}$$

where ω_0 is the natural frequency of small oscillations about the equilibrium point x^* of equation (9), and is given by

$$\omega_0 = \sqrt{k/mL_0}, \tag{11}$$

where

$$k = (\mathrm{d}\bar{f}^e/\mathrm{d}\tilde{x})\,(\tilde{x}^*). \tag{12}$$

Further, one introduces

$$x(t) = \tilde{x}(t/\omega_0), \qquad y(t) = (1/\omega_0)\tilde{y}(t/\omega_0), \qquad \zeta(t) = (1/\gamma)\tilde{\zeta}(t/\omega_0), \tag{13}$$

and equations (9) take the form

$$\dot{x} = y, \qquad \dot{y} = f(x) + \varepsilon\Phi_0\,\zeta + \varepsilon p\cos(\omega t), \qquad \dot{\zeta} = -[1/\gamma\omega_0 + 2y/x]\zeta - 2y/x, \quad (14\text{–}16)$$

where

$$f(x) = -\bar{f}^e(\tilde{x})/k, \qquad \varepsilon\Phi_0 = G_0/k, \qquad \varepsilon p = P/k, \qquad \omega = \Omega/\omega_0, \quad (17)$$

and where superposed dots now represent differentiation with respect to the non-dimensional time t.

Thus, though the oscillator has one degree of freedom, its dynamics is described by a three dimensional state space due to the history dependence of the restoring force.

In what follows, one shall assume that $0 \leqslant \varepsilon \ll 1$ while p and Φ_0 are $\mathcal{O}(1)$. When $\varepsilon = 0$, there is no coupling between equation (15) and equation (16). This leads to a simpler system that will be studied first. One then considers the case $0 < \varepsilon \ll 1$ as a perturbation of the case where $\varepsilon = 0$.

One shall also assume that the dimensionless elastic force is linear, and that it is given by $f(x) \equiv 1 - x$. This is equivalent to assuming $\bar{f}^e(\tilde{x}(\tau)) = -k(\tilde{x}(\tau) - \tilde{x}^*)$ with $\tilde{x}^* = 1$, i.e., since $\tilde{x}^* = 1$ corresponds to the undistorted state of the bar; one is considering small motions about this undistorted state. The problem of weakly non-linear elastic restoring forces may be treated in a manner similar to what will be described in this paper.

3. THE CASE $\varepsilon = 0$

One starts by noting that when $\varepsilon = 0$, the motion is a free (i.e. undamped and unforced) sinusoidal oscillation about the fixed point at $x = 1$. Such a motion may be represented by

$$x_0(t) = 1 + A\cos(\omega t) + B\sin(\omega t), \qquad y_0(t) = -\omega A\sin(\omega t) + \omega B\cos(\omega t), \quad (18, 19)$$

or alternatively in polar form by

$$x_0(t) = 1 + R\cos(\omega t - \Theta), \qquad y_0(t) = -R\sin(\omega t - \Theta), \quad (20, 21)$$

where

$$R = \sqrt{A^2 + B^2}, \qquad \Theta = \arctan(B/A). \quad (22, 23)$$

Note that, though there is no coupling between the evolution equation for $\zeta(t)$, i.e., equation (16), and the governing equations for $x(t)$ and $y(t)$, i.e., equations (14) and (15), $\zeta(t)$ itself is not zero. In fact, a time integration of equation (16) gives†

$$\zeta^u(t) = z_0\frac{x_0^2(t_0)}{x_0^2(t)}\,e^{-(1/\gamma\omega_0)(t - t_0)} + \frac{e^{-(1/\gamma\omega_0)t}}{x_0^2(t)}\int_{t_0}^{t} -2y_0(t')x_0(t')e^{(1/\gamma\omega_0)t'}\,\mathrm{d}t', \quad (24)$$

where the superscript u in ζ^u denotes that this is a solution to the unperturbed problem, (i.e. in the case $\varepsilon = 0$), and where $x_0(t)$ and $y_0(t)$ denote the unforced, undamped solution of equations (14) and (15), which is given by equations (18) and (19), and z_0 denotes the value of $\zeta^u(t)$ at some initial time $t = t_0$. It is clear that the first term of equation (24) is exponentially decaying in time. Therefore, since $x_0(t)$ and $y_0(t)$ are periodic, $\zeta^u(t)$ will eventually be periodic, i.e., after the initial transient has died out. Figure 2 shows such an orbit with $(x(0), y(0), \zeta(0)) = (1{\cdot}1, 0{\cdot}1, 0)$, and $\gamma\omega_0 = 2$.

† Alternatively, this may be obtained from equation (8).

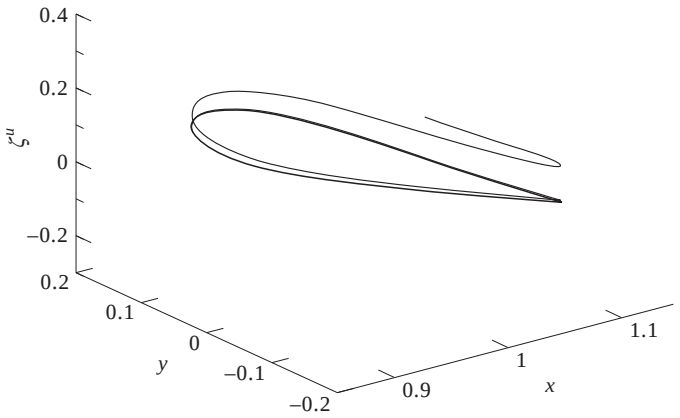

Figure 2. An eventually periodic orbit $(x(t), y(t), \zeta(t))$ of equations (14), (15) and (16) with $\varepsilon = 0$, $(x(0), y(0), \zeta(0)) = (1{\cdot}1, 0{\cdot}1, 0)$, and $\gamma\omega_0 = 2$.

It may be noted that a special choice of the initial value z_0 for $t = t_0$ will directly lead to periodic behavior for $\zeta^u(t)$. Denoting this value of z_0 by z_{0T}, one may write

$$\zeta^u(t_0\,; z_{0T}) = \zeta^u(t_0 + T; z_{0T}), \tag{25}$$

where T denotes the period of $x_0(t)$ and $y_0(t)$. Using the periodicity of $x_0(t)$, this gives

$$z_{0T} = \frac{1}{1 - e^{-(1/\gamma\omega_0)T}} \frac{e^{-(1/\gamma\omega_0)(t_0+T)}}{x_0^2(t_0)} \int_{t_0}^{t_0+T} -2y_0(t')x_0(t')e^{(1/\gamma\omega_0)t'}\,\mathrm{d}t'. \tag{26}$$

One now substitutes equations (20) and (21) into equation (24) and performs the integration. In doing so, one assumes $t_0 = 0$ without loss of generality. One obtains

$$\begin{aligned}\zeta^u(t) = {} & e^{-(1/\gamma\omega_0)t}/(1 + R\cos(\omega t - \Theta))^2 \\ & \times [z_0(1 + R\cos\Theta)^2 + (2\gamma\omega_0\,\omega R/[1 + \gamma^2\omega_0^2\,\omega^2])(\gamma\omega\omega_0\cos\Theta + \sin\Theta) \\ & \times (2R^2\omega\gamma\omega_0/[2 + 8\gamma^2\omega_0^2\,\omega^2])(2\gamma\omega\omega_0\cos 2\Theta + \sin 2\Theta)] \\ & -[2/(1 + R\cos(\omega t - \Theta))^2]((\gamma\omega_0\,\omega R/[1 + \gamma^2\omega_0^2\,\omega^2]) \\ & \times (\gamma\omega_0\,\omega\cos(\omega t - \Theta) - \sin(\omega t - \Theta)) \\ & -\gamma\omega_0\,\omega R^2/([2 + 8\gamma^2\omega_0^2\,\omega^2])(2\gamma\omega_0\,\omega\cos(2\omega t - 2\Theta) - \sin(2\omega t - 2\Theta))).\end{aligned} \tag{27}$$

Clearly, the first term of equation (27) is a transient with exponentially decaying amplitude. Therefore, in the steady state, $\zeta^u(t)$ is given by the second term of equation (27) alone, which has no dependence on the initial value z_0. One may then define $\zeta_0(t)$ as the steady state value of $\zeta^u(t)$ that corresponds to equations (20) and (21), and one has

$$\begin{aligned}\zeta_0(t) = {} & -[2/(1 + R\cos(\omega t - \Theta))^2]((\gamma\omega_0\,\omega R/[1 + \gamma^2\omega_0^2\,\omega^2])(\gamma\omega_0\,\omega\cos(\omega t - \Theta) \\ & -\sin(\omega t - \Theta)) - (\gamma\omega_0\,\omega R^2/[2 + 8\gamma^2\omega_0^2\,\omega^2])(2\gamma\omega_0\,\omega\cos(2\omega t - 2\Theta) - \sin(2\omega t - 2\Theta))).\end{aligned} \tag{28}$$

4. THE CASE $0 < \varepsilon \ll 1$

In order to look for solutions of equations (14–16) in the case where $\varepsilon \neq 0$ the method of variation of parameters will be used (see e.g., references [13, 11, 14]). Thus one expects, for ε sufficiently small, that there will be a periodic solution of equations (14–16) that is of the same form as equations (18) and (19), but with the constants A and B replaced by time dependent coefficients $u(t)$ and $v(t)$. For this motion, one writes

$$x(t) = 1 + u(t)\cos(\omega t) + v(t)\sin(\omega t), \qquad y(t) = -\omega u(t)\sin(\omega t) + \omega v(t)\cos(\omega t). \tag{29, 30}$$

For later use, one notes that in polar co-ordinates, this corresponds to

$$x(t) = 1 + r(t)\cos(\omega t - \phi(t)), \qquad y(t) = -\omega r(t)\sin(\omega t - \phi(t)), \tag{31, 32}$$

where $r(t)$ and $\phi(t)$ replace the constants R and Θ respectively in equations (20) and (21). It also follows that

$$u(t) = r(t)\cos(\phi(t)), \qquad v(t) = r(t)\sin(\phi(t)). \tag{33, 34}$$

Next, solving for $u(t)$ and $v(t)$ from equations (29) and (30), differentiating the resulting expressions, and using equations (14) and (15) gives the dynamical equations for the evolution of $u(t)$ and $v(t)$. These are

$$\dot{u} = -\omega[(x-1)(1-1/\omega^2) + (\varepsilon/\omega^2)\Phi_0\,\zeta(t) + (\varepsilon/\omega^2)p\cos(\omega t)]\sin(\omega t), \tag{35}$$

$$\dot{v} = -\omega[(x-1)(1-1/\omega^2) + (\varepsilon/\omega^2)\Phi_0\,\zeta(t) + (\varepsilon/\omega^2)p\cos(\omega t)]\cos(\omega t). \tag{36}$$

For what follows, it is convenient to use polar co-ordinates. Thus, using equations (33) and (34) in equations (35) and (36), one obtains

$$\dot{r} = F_1\cos(\phi) + F_2\sin(\phi), \qquad \dot{\phi} = (1/r)(F_2\cos(\phi) - F_1\sin(\phi)), \tag{37, 38}$$

where

$$F_1 = -\omega[r(t)\cos(\omega t - \phi(t))(1-1/\omega^2) + (\varepsilon/\omega^2)\Phi_0\,\zeta(t) + (\varepsilon/\omega^2)p\cos(\omega t)]\sin(\omega t), \tag{39}$$

$$F_2 = -\omega[r(t)\cos(\omega t - \phi(t))(1-1/\omega^2) + (\varepsilon/\omega^2)\Phi_0\,\zeta(t) + (\varepsilon/\omega^2)p\cos(\omega t)]\cos(\omega t). \tag{40}$$

The use of variation of parameters for $\zeta_0(t)$ in equation (28) gives

$$\zeta(t) = -\frac{2}{(1 + r(t)\cos(\omega t - \phi(t)))^2} \times \left(\frac{\gamma\omega_0\,\omega r(t)}{1 + \gamma^2\omega_0^2\,\omega^2}(\gamma\omega_0\,\omega\cos(\omega t - \phi(t)) - \sin(\omega t - \phi(t))) - \frac{\gamma\omega_0\,\omega r(t)^2}{2 + 8\gamma^2\omega_0^2\,\omega^2}(2\gamma\omega_0\,\omega\cos(2\omega t - 2\phi(t)) - \sin(2\omega t - 2\phi(t))) \right), \tag{41}$$

which is to be substituted into equations (39) and (40).

For ω close to 1, equations (37) and (38) are in a form that allows for the method of averaging to be employed to determine the existence and stability of $r(t)$ and $\phi(t)$. (For a discussion of the method of averaging, see for example references [14], [11], pages

166–180].) Averaging equations (37) and (38) over one period, i.e., $2\pi/\omega$, one obtains

$$\dot{\bar{r}} = \frac{\varepsilon\pi}{\bar{r}\sqrt{1-\bar{r}^2}\omega^2}\left[\frac{-2\gamma\omega_0\,\omega\Phi_0}{2+8\gamma^2\omega_0^2\,\omega^2}(-8+(4+2\bar{r}^2+4\sqrt{1-\bar{r}^2})(1+\cos 2\overline{\phi}+\sin 2\overline{\phi}))\right.$$

$$\left. -\frac{4\gamma\omega_0\,\omega\Phi_0}{1+\gamma^2\omega_0^2\,\omega^2}(1-\sqrt{1-\bar{r}^2})+p\bar{r}\sqrt{1-\bar{r}^2}\sin\overline{\phi}\right], \tag{42}$$

$$\dot{\overline{\phi}} = \frac{\varepsilon\pi}{\bar{r}^4(1-\bar{r}^2)^{3/2}\omega^2}\left[\frac{-2\gamma\omega_0\,\omega\Phi_0}{2+8\gamma^2\omega_0^2\,\omega^2}[(4-6\bar{r}^2+2\bar{r}^4-4(1-\bar{r}^2)^{3/2})(-1+4\gamma\omega_0\,\omega)\right.$$

$$-4\gamma\omega_0\,\omega\bar{r}^4+(4+6\bar{r}^2-2\bar{r}^4+4(1-\bar{r}^2)^{3/2})(\cos 2\overline{\phi}-\sin 2\overline{\phi})+8\sin 2\overline{\phi}]$$

$$\left.+\bar{r}^4(1-\bar{r}^2)^{3/2}(\omega^2-1)-\frac{4\gamma^2\omega_0^2\,\omega^2\Phi_0\,\bar{r}^2}{1+\gamma^2\omega_0^2\,\omega^2}[-1+\bar{r}^2+(1-\bar{r}^2)^{3/2}]\right], \tag{43}$$

where $\bar{r}$ and $\overline{\phi}$ denote the averages of r and ϕ, respectively.

It follows from the Averaging Theorem that for sufficiently small ε, an equilibrium point of the averaged equations (42) and (43) corresponds to a periodic orbit of equations (37) and (38) and, therefore, of the original dynamical equations (14–16). In Figure 3, the value of $\bar{r}$ for such equilibrium points is plotted as a function of the angular frequency ω for three different values of the relaxation modulus Φ_0. As one would expect, larger values of Φ_0 lead to smaller amplitudes due to larger dissipation. The corresponding phase lag $\overline{\phi}$ is shown in Figure 4.

In Figures 5 and 6, the value of $\bar{r}$ and $\overline{\phi}$ of the equilibrium points of equations (42) and (43) are shown as functions of ω for various values of $\gamma\omega_0$ and fixed Φ_0. Figure 5 shows that, as $\gamma\omega_0$ is decreased, the maximum value of $\bar{r}$ occurs at a value of ω which approaches 1. On the other hand, an increase in $\gamma\omega_0$, which corresponds to an increasing importance of memory effects, results in the maximum of the amplitude curve being shifted to the right.

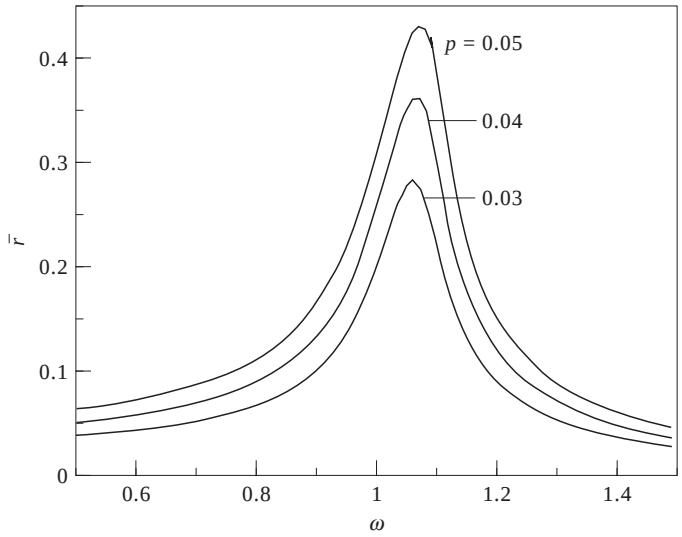

Figure 3. Amplitude dependence of harmonic response for various values of p; $\Phi_0 = 0{\cdot}1$, $\gamma\omega_0 = 1$.

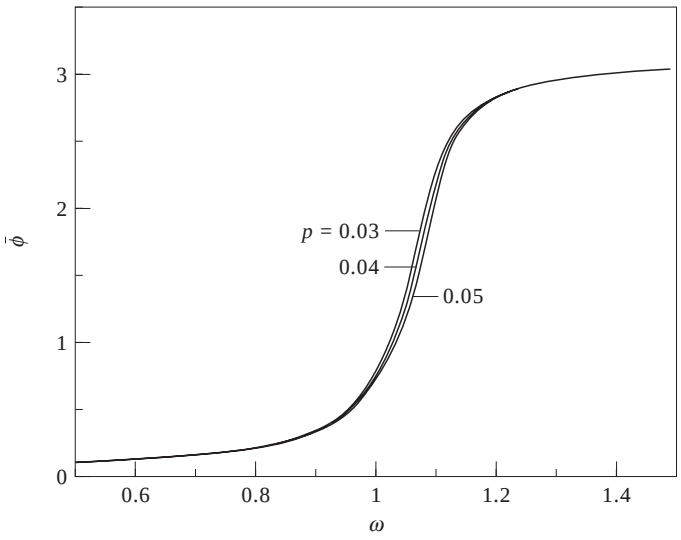

Figure 4. Phase dependence of harmonic response for various values of p; $\Phi_0 = 0{\cdot}1$, $\gamma\omega_0 = 1$.

At the same time, the curves tend to "fold" to the right in a way similar to that typical of a hardening spring.

Figures 7 and 8 show two saddle–node bifurcations for the equilibrium of equations (42) and (43). These occur for the values of $\omega \approx 1{\cdot}20$ and $\omega \approx 1{\cdot}26$. In the region between these saddle–node bifurcations, there are three (two stable and one unstable) coexisting equilibria. How well these bifurcations reflect bifurcations that occur in the periodic orbits of equations (14–16) is commented on in the next section.

A phase portrait of equations (42) and (43) showing the two stable fixed points and the unstable saddle point that are created through the saddle–node bifurcations in Figures 7 and 8 is shown in Figure 9. The curves are the invariant manifolds of the saddle point

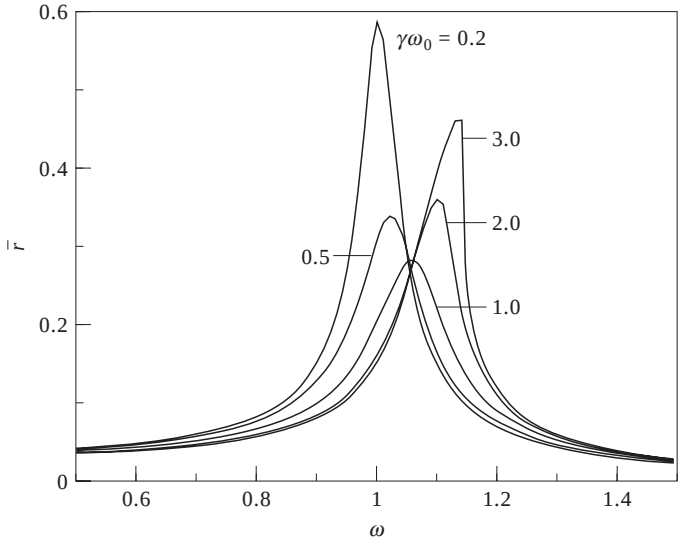

Figure 5. Amplitude dependence of harmonic response for various values of $\gamma\omega_0$; $\Phi_0 = 0{\cdot}1$, $p = 0{\cdot}03$.

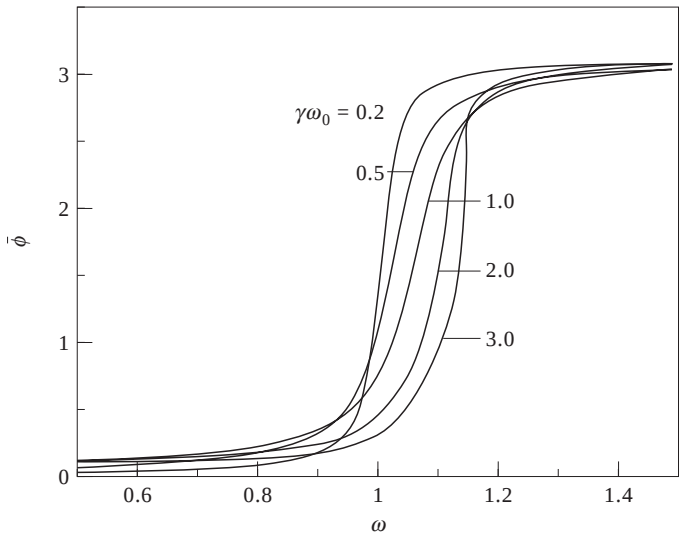

Figure 6. Phase dependence of harmonic response for various values of $\gamma\omega_0$; $\Phi_0 = 0{\cdot}1$, $p = 0{\cdot}03$.

at $(\bar{r}, \bar{\phi}) \approx (0{\cdot}74, 2{\cdot}1)$. The stable fixed points are at $(\bar{r}, \bar{\phi}) \approx (0{\cdot}35, 2{\cdot}8)$ and $(\bar{r}, \bar{\phi}) \approx (0{\cdot}78, 1{\cdot}2)$. The two corresponding coexisting periodic orbits of equations (14–16) are shown in Figure 10.

5. DISCUSSION: LIMITATIONS OF AVERAGING RESULTS

When $\bar{r}$ (which may serve as an approximation for the amplitude of the non-linear periodic motion of equations (14, 15)) approaches 1, $\zeta_0(t)$ defined in equation (28) is no longer $\mathcal{O}(1)$, so that $\varepsilon\zeta_0(t)$ may not be considered small. The results obtained by the method of averaging are then not strictly valid, though they may give a good qualitative indication

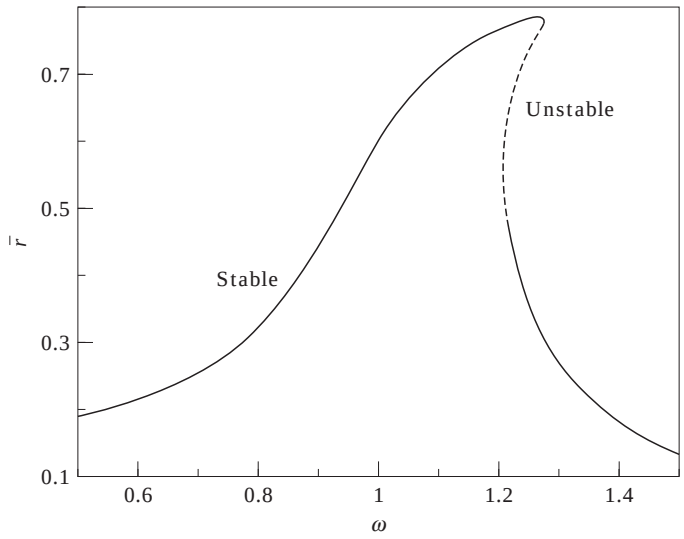

Figure 7. Example of a jump bifurcation that may occur in the amplitude for an oscillator with history dependent damping; $\gamma\omega_0 = 1{\cdot}0$, $\Phi_0 = 0{\cdot}1$, $p = 0{\cdot}15$.

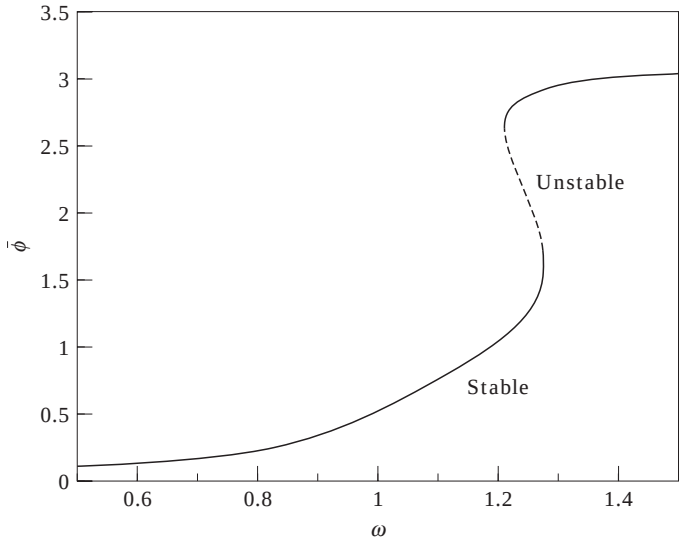

Figure 8. Example of a jump bifurcation that may occur in the phase angle for an oscillator with history dependent damping; $\gamma\omega_0 = 1{\cdot}0$, $\Phi_0 = 0{\cdot}1$, $p = 0{\cdot}15$.

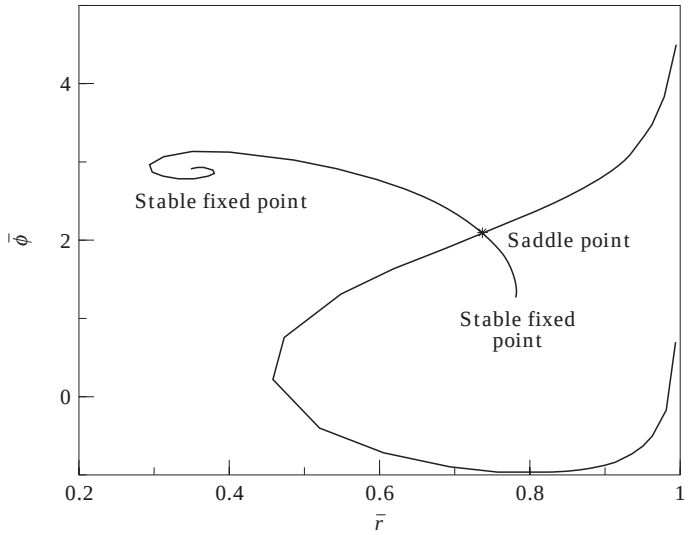

Figure 9. Phase portrait of the averaged system for $\gamma\omega_0 = 1{\cdot}0$, $\omega = 1{\cdot}25$, $\varepsilon p = 0{\cdot}15$, and $\varepsilon\Phi_0 = 0{\cdot}10$.

of the behavior of the system. As an illustration, the amplitude curve in Figure 7 may be compared to an amplitude curve numerically obtained by the use of the "brute force" method†. Thus, defining an approximation for the amplitude of the periodic orbit for a certain value of ω by $\xi = x_{max} - 1$, where x_{max} is the maximum value of x on the periodic orbit for that value of ω, such a bifurcation diagram is obtained for ξ and is shown in Figure 11 (dots). For the sake of comparison, the amplitude curve of Figure 7, which is

† In the brute force method, the stable periodic orbit is determined numerically for a sequence of values of ω and, for example, the maximum x value on each orbit is plotted against the corresponding value of ω. The resulting plot gives an indication of the existence of the orbit and its amplitude for the range of values of ω considered (see e.g., reference [15]).

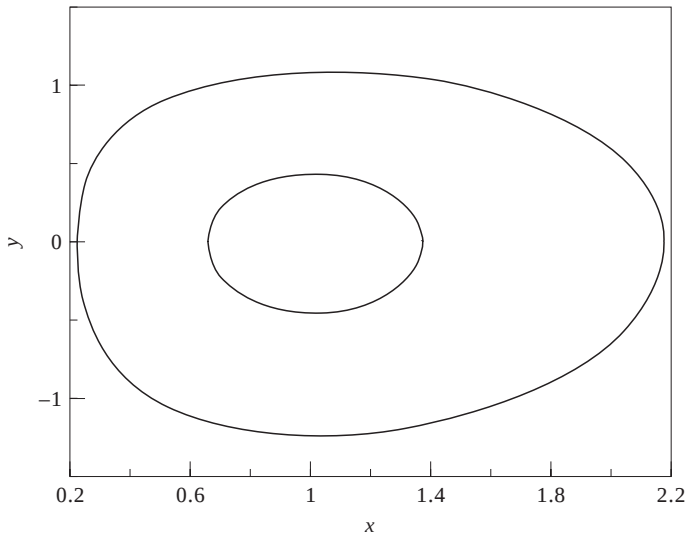

Figure 10. The two coexisting periodic orbits of different amplitude at $\varepsilon p = 0{\cdot}15$, $\gamma\omega_0 = 1{\cdot}0$, $\varepsilon\Phi_0 = 0{\cdot}1$, $\omega = 1{\cdot}25$.

obtained by the method of averaging, is shown in the same diagram (solid curve). Note that the two amplitude curves do not agree well when the amplitude of the periodic orbit is larger than approximately 0·6. However, the prediction of a saddle–node bifurcation at $\omega \approx 1{\cdot}2$ given by Figure 7 is accurate since this bifurcation occurs at an amplitude of approximately 0·6. On the other hand, the saddle–node bifurcation predicted by Figure 7 to occur at $\omega = 1{\cdot}27$ occurs in fact for $\omega \approx 1{\cdot}22$. Note that since the "brute force" method cannot capture unstable orbits, the saddle–node bifurcations appear as jump bifurcations.

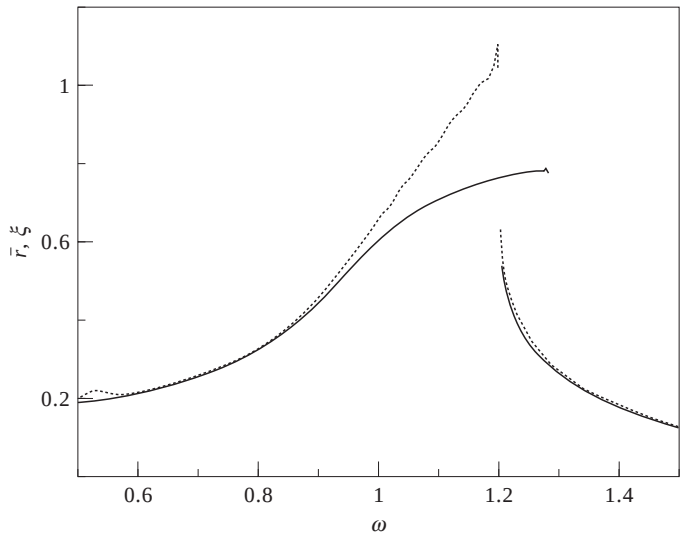

Figure 11. A comparison between the amplitude of oscillations $\bar{r}$ as obtained by the method of averaging and shown in Figure 7 (——), and a bifurcation diagram obtained by the "brute force" method (· · · ·). (The unstable branch in Figure 7 is not shown.) $\gamma\omega_0 = 1{\cdot}0$, $\Phi_0 = 0{\cdot}1$, $p = 0{\cdot}15$.

6. CONCLUDING REMARKS

Most currently used models for the dynamic mechanical behavior of viscoelastic materials are based on frequency dependent complex moduli. These models are adequate for linear oscillations. In the case of large vibrations, the non-linear dependence of the viscoelastic force on the history of the motion becomes of importance. An understanding of this non-linear behavior may widen the scope of applications of viscoelastic materials.

A possible description of the effects of non-linear history dependence is given by the material-with-memory model. The adequacy of this model in describing true viscoelastic behavior strongly depends on the relaxation function used. In this paper, the simple exponentially decaying relaxation function with a single relaxation time was adopted. This may serve as a general model for some materials, and even in cases where a viscoelastic material is not strictly described by this relaxation function, the results may serve as an indication of what qualitative behavior to expect. However, a continued study of the dynamics of systems with non-linear history dependence, with more complex relaxation functions, remains important.

REFERENCES

1. A. D. Nashif, D. I. G. Jones and J. P. Henderson 1985 *Vibration Damping*. John Wiley.
2. A. Okazaki, Y. Urata and A. Tatemichi 1990 *Japan Society of Mechanical Engineers International Journal*, Series I, **33**, 145–151. Damping properties of a three layered shallow spherical shell with a constrained viscoelastic layer.
3. B. P. Gautham and N. Ganesan 1994 *Journal of Sound and Vibration* **170**, 289–301. Vibration and damping characteristics of spherical shells with a viscoelastic core.
4. P. M. Culkowski and H. Reismann 1971 *Journal of Sound and Vibration* **14**, 229–240. The spherical sandwich shell under axisymmetric static and dynamic loading.
5. D. F. Moore 1993 *Viscoelastic Machine Elements*. Butterworth-Heinemann.
6. B. D. Coleman 1964 *Archive for Rational Mechanics and Analysis* **17**, 1–46. Thermodynamics of materials with memory.
7. C. Truesdell and W. Noll 1965 *Handbook of Physics* **III**/3. New York: Springer-Verlag. The non-linear field theories of mechanics.
8. R. L. Fosdick, Y. Ketema and J. H. Yu 1997 *International Journal of Solids and Structures*. In press. Vibration damping through the use of materials with memory.
9. Y. M. Haddad 1995 *Viscoelasticity in Engineering*. Chapman and Hall. Materials.
10. R. L. Fosdick, Y. Ketema and J. H. Yu 1997 *International Journal of Nonlinear Mechanics* (In press). A nonlinear oscillator with history dependent forces.
11. J. Guckenheimer and P. Holmes 1983 *Applied Mathematical Sciences* **42**. Berlin: Springer-Verlag. Nonlinear oscillations, dynamical systems, and bifurcation of vector fields.
12. B. D. Coleman and W. Noll 1961 *Reviews of Modern Physics* **33**, 239–249. Foundations of linear viscoelasticity.
13. M. Braun 1984 *Applied Mathematical Sciences* **15**. New York: Springer-Verlag. Differential equations and their applications.
14. A. H. Nayfeh 1993 *Introduction to Perturbation Techniques*. John Wiley.
15. T. S. Parker and L. O. Chua 1989 *Practical Numerical Algorithms for Chaotic Systems*. New York: Springer-Verlag.